



## Environmental NMR: High-resolution Magic-angle Spinning

Ruth E. Stark<sup>1,2</sup>, Bingwu Yu<sup>1,2</sup>, Junyan Zhong<sup>1</sup>, Bin Yan<sup>1,2</sup>, Guohua Wu<sup>1</sup> & Shiyong Tian<sup>1</sup>

<sup>1</sup>College of Staten Island, City University of New York, New York, NY, USA

<sup>2</sup>City College of New York, City University of New York, New York, NY, USA

Environmentally significant materials including soils, plant tissues, melanin pigments, and urban surface films possess swollen or swellable constituents that are not studied ideally using either solution- or solid-state NMR. Beginning in the 1970s and accelerating during the past 15 years, high-resolution (HR)-MAS techniques have been developed to study these challenging materials, yielding unprecedented molecular detail and informing mechanistic hypotheses. This valuable information has been forthcoming without the need for soil or tissue extraction, and without subjecting the macromolecular entities of interest to chemical degradation. In this overview, we focus on practical HR-MAS NMR strategies, including both methodological fundamentals and illustrative architectural findings for soil organic matter, plant protective polymers and biomass, and ultraviolet-resistant melanin pigments. In addition to the acquisition of one-dimensional spectra tailored for mobile or immobilized constituents of whole soils, we illustrate the use of HR-MAS in conjunction with two-dimensional NMR experiments [COSY, TOCSY, heteronuclear multiple-quantum coherence (HMQC), and heteronuclear multiple-bond correlation (HMBC)] to elucidate the macromolecular chemistry of terrestrial plant litter decomposition and environmental stress resistance at plant surfaces.

**Keywords:** NMR, magic-angle spinning, HR-MAS, environmental, soil, plant, suberin, cutin, carbon cycling

### How to cite this article:

*eMagRes*, 2013, Vol 2: 377–388. DOI 10.1002/9780470034590.emrstm1340

### Introduction

Traditionally, most NMR investigations of molecular structure and dynamics have been conducted on samples in solution or the solid state. However, these well-developed and information-rich spectroscopic approaches are frequently ill suited to intermediate states such as liquid crystals, bulk polymers, or colloidal dispersions. Materials of interest in environmental science, such as soils, plant tissues, melanin pigments, and urban surface films, have major swollen or swellable constituents that are not studied ideally using either solution- or solid-state NMR alone. On the one hand, partial orientational order or overall tumbling that is restricted in terms of rate and/or angular excursion may render motional narrowing incomplete, compromising both spectral resolution and sensitivity in solution-state NMR experiments. These same characteristics may compromise the efficiency of CP in solid-state experiments; moreover, the resolution and consequent structural details of the latter spectra may prove disappointing, even with MAS, if the samples are amorphous rather than microcrystalline. Thus, to examine the molecular structure and motion of such materials in their intact 'native' states, strategies that select or combine the advantages of particular solution- and solid-state methods to obtain high-quality NMR data are desirable.

<sup>1</sup>H MAS NMR approaches were reported as early as the 1970s for solvent-swollen cross-linked polystyrene gels<sup>1,2</sup> and extended a decade later to obtain <sup>13</sup>C spectra using direct polarization (DP) in combination with MAS methods for solvated, mobile macromolecular moieties that exhibit partially

averaged dipolar interactions and chemical-shift anisotropy.<sup>3</sup> In contrast to the weak CP-MAS <sup>13</sup>C NMR signals observed for such materials,<sup>4</sup> DP-MAS experiments conducted with very modest decoupling strengths (~3 kHz) and spin rates (~2 kHz) yielded well-resolved resonances for both backbone chains and cross-link junctions. The latter approach opened up new ways to monitor chemical functionalization, in situ gelation kinetics, and cross-link morphology.<sup>5</sup>

The late 1980s also witnessed the introduction of MAS NMR methods for spectral observation of lyotropic liquid crystals such as model biological membranes,<sup>6,7</sup> in which rapid lateral diffusion and axial rotation reduce inter- and intramolecular dipole–dipole interactions, respectively. This breakthrough made it possible to obtain high-resolution <sup>1</sup>H, <sup>13</sup>C, and <sup>31</sup>P spectra of multibilayers without sonication, laying the groundwork for subsequent extensions of this strategy. For instance, <sup>13</sup>C MAS NMR spectra were resolved and assigned for cell-wall glucans in whole yeast cells,<sup>8</sup> and two-dimensional (2-D) MAS-assisted NOESY measurements were used to investigate the bilayer organization of phospholipid multibilayers<sup>9</sup> and the partitioning of ethanol within such model biological membranes.<sup>10</sup>

Spurred in part by the high-throughput demands of combinatorial chemistry, this period also saw a significant advance that was dubbed high-resolution (HR)-MAS, achieved by the engineering of NMR probes to average discontinuities in bulk magnetic susceptibility. The HR-MAS technology was applied first in a Nano-NMR<sup>®</sup> probe to characterize peptides and drug candidates that were still covalently attached to the

solvent-swelled polymeric resins used in solid-phase organic synthesis<sup>11</sup> and subsequently extended with PFGs and diverse probe designs to obtain 2-D homo- and heteronuclear correlated NMR spectra that permitted structural elucidation.<sup>12–14</sup> Beginning later in the 1990s, HR-MAS capabilities were also exploited extensively to assist in characterization of diseased human tissue samples and other biomedical targets.<sup>15</sup>

In the environmental science and agricultural fields, early applications of one-dimensional (1-D) and 2-D HR-MAS NMR included studies of stress-resistant plant tissues<sup>16</sup> dispersed in aqueous and organic solvents, respectively.<sup>16</sup> The usefulness of HR-MAS NMR methods has also been recognized for structural investigations of soil samples<sup>17</sup> and melanin pigments.<sup>18</sup> Recent reviews including HR-MAS NMR applications have focused on applications to live bacterial cells,<sup>19</sup> food science,<sup>20</sup> biomedical metabolomics,<sup>21</sup> and environmental science.<sup>22</sup> Unprecedented molecular information, often with diagnostic or biochemical significance, has thus been forthcoming without the need for, e.g., isolation of cellular extracts or chemical degradation of the constituent biopolymers. The NMR strategies required to achieve such results are the principal subject of this overview, in which both fundamentals of the HR-MAS technique and the resulting atomic-level findings are illustrated for environmentally important targets including soil organic matter, protective plant polymers, and ultraviolet (UV)-resistant melanin pigments.

## Experimental Methods

The following section outlines the experimental procedures required to obtain well-resolved, high-sensitivity HR-MAS NMR spectra that fairly represent the chemical moieties in swelled solids, using plant biopolymers and biomass, fungal melanin, and whole soil samples to illustrate these guidelines.

### Validation of <sup>1</sup>H HR-MAS NMR Spectra for Intractable Environmental Solids

The impressive resolution enhancement achieved by solvent swelling combined with MAS-assisted NMR acquisition is illustrated in Figure 1, which compares <sup>1</sup>H MAS NMR spectra of an insoluble plant polymer from intact lime fruit (*Citrus aurantifolia*) cuticle in dry and swelled states.<sup>23,24</sup> The relatively featureless 300 MHz spectrum of dry cutin (>100 Hz full width at half height for (CH<sub>2</sub>)<sub>n</sub> groups) obtained with what was, at the time, considered moderately rapid 12 kHz MAS (red trace) is narrowed by at least 70% if the sample is swelled in DMSO-*d*<sub>6</sub>, but observed using slower 8 kHz HR-MAS (green inset). Moreover, the quantitative reliability of spectra obtained for this 'soggy' solid may be validated by establishing that all of the resonances observed using MAS on dry samples are represented in their correct amounts and proportions using the alternative of MAS applied to solvent-swelled materials. Thus, if 70 Hz of artificial broadening is applied to the spectrum of the swelled lime cutin sample, it becomes nearly coincident with dry cutin (blue trace). This result shows that solvent swelling has reduced the linewidths but preserved both the absolute integrated signal intensity and the relative ratios of the components

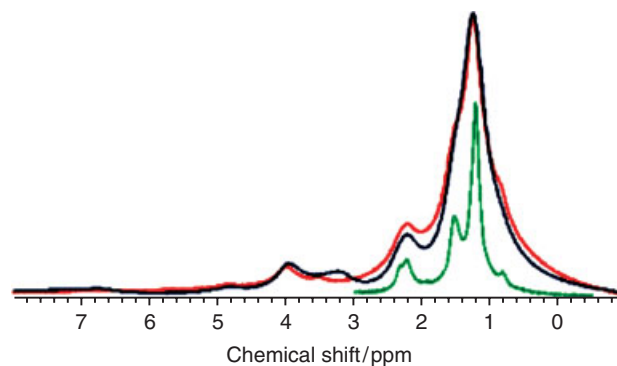


**Figure 1.** 300 MHz <sup>1</sup>H HR-MAS NMR spectra of an intact lime fruit cutin polymer, as either a dry powder spinning at 12 kHz (red) or a dispersion of 11 mg cutin swelled in ~60 mg DMSO-*d*<sub>6</sub> and spinning at 8 kHz (green, no artificial line broadening; blue, 70 Hz exponential line broadening). The data were obtained using a Doty XC-5 probe and presented, in part, previously<sup>24</sup>

derived from the spectrum. Stated differently, solvent swelling increases the effective <sup>1</sup>H spin–spin relaxation times (*T*<sub>2</sub>) but yields a similar spectroscopic fingerprint corresponding to the macromolecular structure of the cutin polymer.

Using a probe with optimized <sup>1</sup>H lineshape characteristics and collecting the NMR data at 600 MHz, it is possible to observe aliphatic resonances for the swelled polymer with resolution that approaches that achieved for a soluble constituent trimeric fragment (Figure 2).<sup>24</sup> Both spectra provide straightforward estimates of the types and numbers of functional groups that comprise this intractable plant material. For instance, in the polymer, a variety of aliphatic components [–CH<sub>3</sub> at 0.9 ppm, 3H; –(CH<sub>2</sub>)<sub>n</sub>– at 1.2 and 1.5 ppm, 42H; –CH<sub>2</sub>COO– and –CH<sub>2</sub>C(O)CH<sub>2</sub>– at 2.2–2.4 ppm, 6H; –CH<sub>2</sub>OR or –CHOH at 3.4 ppm (set to 1H); and CH<sub>2</sub>OC(O) at 4.0 ppm, 3H] are fairly well resolved. It is also possible to discern modest spectral contributions from multiply bonded groups (5.5–6.0 ppm). Other than the latter moieties, these results fit the compositional profile derived from an extensive series of <sup>13</sup>C solid-state NMR measurements on the dry material,<sup>25–27</sup> thus confirming that most functional groups in lime fruit cutin are rendered flexible enough to display <sup>1</sup>H NMR signals under conditions of solvent swelling and slow MAS. Similar approaches have also been adopted for structural investigations of cutins from tomato fruits and *Agave americana* leaves.<sup>28,29</sup>

The potential of HR-MAS experiments conducted on swelled solids is also demonstrated by the PFG-assisted 2-D hetero-correlated multiple-quantum coherence (HR-MAS-gHMQC) spectra<sup>30</sup> in Figure 3, which are acquired as straightforwardly as their solution-state analogs and again show excellent resolution.<sup>16,24</sup> The somewhat broader contours of the polymer spectrum, which parallel the broader linewidths noted in the 1-D spectra of Figure 2, are attributed to chemical-shift heterogeneity rather than incomplete motional averaging, because the intact cutin likely contains a greater variety of chemically and magnetically similar moieties as compared with a trimeric fragment obtained by low-temperature hydrofluoric acid treatment. A discussion of how HR-MAS can complement

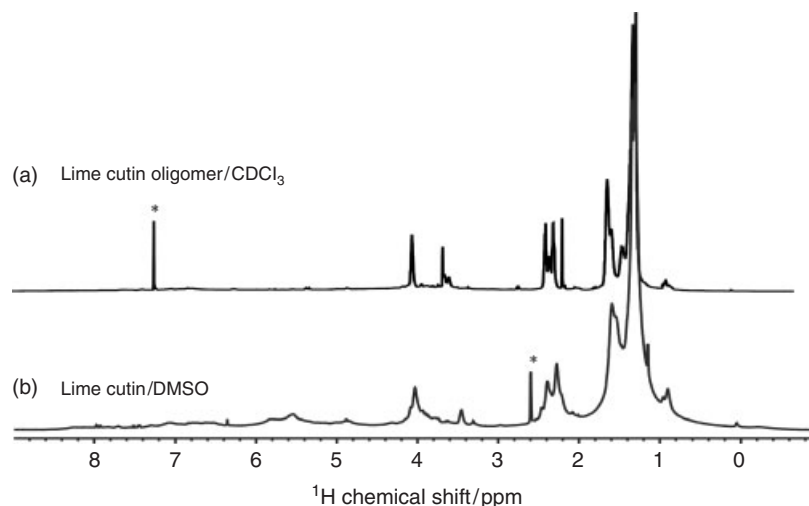


**Figure 2.** An oligomer obtained by chemical degradation of the polymer (a) and 600 MHz  $^1\text{H}$  HR-MAS NMR spectra of an intact lime fruit cutin polymer swelled in  $\text{DMSO-}d_6$  at  $50^\circ\text{C}$  (b)<sup>24</sup>. The spectra were obtained using a Varian (Agilent) nanoprobe with MAS at  $2.500 \pm 0.005$  kHz. The \* designations indicate sharp solvent resonances

solution-state NMR to monitor the associated chemical transformations is presented in the section titled ‘Representative Applications to Environmental Science’.

### Sample Preparation of Swelled Solids

The encouraging results illustrated previously for fruit cuticular polymers nevertheless raise a variety of questions regarding the choice of experimental conditions in HR-MAS NMR experiments. First and foremost, care must be observed regarding the physical state of the solid under study. As noted earlier, near-solution-state resolution in HR-MAS NMR spectra requires partial motional averaging by rapid liquid-like molecular tumbling ( $\geq 10^6 \text{ s}^{-1}$ ); vigorous motions are also expected to lengthen  $^1\text{H}$  and  $^{13}\text{C}$  spin–spin relaxation times ( $T_2$ ) under these circumstances. In practice, attaining values of  $T_2^{\text{H}}$  that exceed  $\sim 50$  ms is especially crucial to the success of gradient-assisted 2-D heterocorrelated multiple-bond correlation (MAS-gHMBC) experiments: their three-bond and four-bond correlations are richly informative regarding molecular structure, but the  $1/2J_{\text{CH}}$  mixing period is vulnerable to signal losses if transverse relaxation occurs too efficiently. This same challenge is well established for HMBC experiments in large protein complexes in solution,<sup>31</sup> for which selective or perdeuteration is used to lengthen the transverse spin relaxation times.

**Surface Area and Solvent Accessibility.** To enhance the overall molecular motion and HR-MAS signal intensity, for instance, the maximum possible surface area of the sample should be exposed to the solvent. Figure 4 compares MAS-assisted HMBC results for the defensive biopolymer suberin formed in potato (*Solanum tuberosum* L.) tuber wound periderms,<sup>16,23</sup> showing differences depending on whether the sample is in flaked or powder form and whether one examines the light- or heavy-powder fractions produced by benchtop centrifugation of a slurried sample. In each case, the resulting HR-MAS NMR

spectra are expected to reflect only solvent-accessible molecular moieties; the soluble portion of the swelled sample should also be examined to rule out contributions from extractable small molecules or degradation products.

The trend for wound-healing suberized potato tissues is clear-cut: the smaller the particles that are dispersed in solution are, the more  $^1\text{H}$ – $^{13}\text{C}$  HMBC NMR cross-peaks are observed with significant intensity. The beneficial effect of increasing surface area-to-volume ratio is especially pronounced for aromatic moieties (solid box:  $\delta_{\text{H}} = 6\text{--}8$  ppm,  $\delta_{\text{C}} = 110\text{--}160$  ppm), which are expected to occur in regions of the polymer-cell-wall matrix that are heavily cross-linked and marginally accessible to solvent. Major enhancements are also observed for the polysaccharide resonances (dashed box:  $\delta_{\text{H}} = 4\text{--}5.5$  ppm,  $\delta_{\text{C}} = 60\text{--}105$  ppm): although their hydrophilic hydroxyl groups could have an affinity for  $\text{DMSO-}d_6$ , their ability to cross-link with the biopolyester could limit solvent accessibility. As detailed in the section titled ‘Representative Applications to Environmental Science’, such optimization measures make it possible, although still challenging, to obtain otherwise inaccessible information regarding macromolecular structure from MAS-assisted 2-D NMR experiments.

**Sample Concentration.** A different potato biopolymer material illustrates a seemingly counterintuitive guideline for the preparation of samples to enhance the signal intensity in these HR-MAS NMR experiments. Although it is tempting to use the highest possible concentration except in sample-limited circumstances, the series of gHMBC NMR spectra in Figure 5 belie this strategy. While raising the concentration at first gives the expected rise in cross-peak intensity, increases beyond  $5 \text{ mg}/50 \mu\text{l}$  have the opposite effect for this sample, an aliphatic–aromatic polymer associated with textural defects in potatoes (*S. tuberosum* L.).<sup>32</sup> The deleterious impact of high concentration on signal strength is especially severe in the aromatic region; as noted for potato suberin, a falloff in intensity

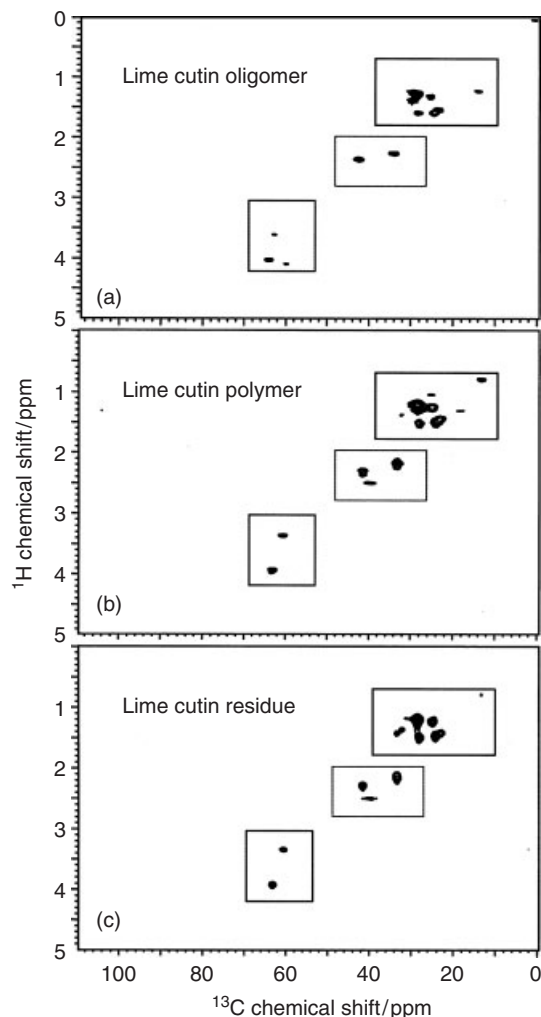


**Figure 3.** 600 MHz  $^1\text{H}$  HR-MAS-gHMBC NMR spectra of intact lime fruit cutin and an associated trimer derived from low-temperature HF degradation,<sup>24,46</sup> displayed as contour plots to obtain a fingerprint for each material. The spectra were obtained with 2.500 kHz MAS and z-axis PFGs of  $11\text{ G cm}^{-1}$ . (a)  $\sim 1$  mg of oligomer dissolved in  $\text{CDCl}_3$  at room temperature. (b) 1.5 mg of polymer swelled in  $40\ \mu\text{l}$  of  $\text{DMSO-}d_6$  at  $50^\circ\text{C}$ . (c) 1.5 mg of insoluble residue from HF treatment swelled in  $40\ \mu\text{l}$  of  $\text{DMSO-}d_6$  at  $50^\circ\text{C}$ . Boxes highlight the oxygenated, carboxylated, bulk methylene, and methyl groups, respectively, as labeled. (Reproduced with permission from Ref. 24. © Elsevier, 2001)

is expected for functional groups that exhibit limited motional freedom.

To put the particle size and concentration trends on a more quantitative footing, spin relaxation measurements were conducted on an insoluble swelled biological solid before and after mechanical grinding; in this case, a  $^{13}\text{C}$ -enriched sample of melanized cell walls from the pathogenic fungus *Cryptococcus neoformans*.<sup>18,33</sup> Like other melanin pigments with roles in soil bioremediation and animal camouflage, this intractable amorphous material is an energy transducer that can either protect living organisms or damage their DNA under different circumstances.<sup>34</sup> Preparation of *C. neoformans* melanin ‘ghosts’

as fine powders enhances the signal-to-noise ratio of MAS-gHMBC NMR spectra by an order of magnitude (data not shown), suggesting explanations that invoke faster tumbling of smaller particles and/or more complete solvent infusion.

The  $T_2^{\text{H}}$  values are surprisingly insensitive to the grinding procedure (Table 1), however, suggesting that faster molecular reorientation of smaller particles is balanced by detection of an additional population of semi-mobile macromolecular species or intermolecular association effects in these ‘soggy’ samples. Nonetheless, the  $T_2^{\text{H}}$  values for aliphatic groups associated with fungal melanins are long enough with respect to typical HMBC defocusing periods of 65 ms to avoid devastating losses in signal intensity, although the aromatic moieties of the pigment (and of plant suberins, data not shown) are more vulnerable to signal losses in such experiments. By contrast, grinding of the melanin sample lengthens  $T_2^{\text{C}}$  values by factors of 12–18 to approach the defocusing time (Table 2), offering possible additional contributions to improved HMBC performance.

**Solvent Choice.** A third consideration in sample preparation concerns the choice of solvent. If the hydrophobic–hydrophilic balance of an intractable solid is uncertain, then DMSO is viewed as a safe compromise choice that is compatible with, e.g., hydrocarbon chains, peptides, polysaccharides, and phenolic ring structures—presuming that such molecular groupings are actually accessible to the solvent. To maximize molecular mobility, a solvent with low viscosity is preferred; this rationale has been exploited, for instance, in high-resolution NMR studies of proteins encapsulated in reverse micelles dissolved in liquid alkanes.<sup>35,36</sup> If a low-viscosity solvent is not suitable for swelling the solid of interest, then it may be practical to enhance molecular mobility by selecting a nonvolatile solvent and running the experiments at the highest temperatures consistent with the probe specifications and sample integrity.

In our experience with the primarily aliphatic cross-linked polyester in lime fruit cutin, both  $\text{DMSO-}d_6$  and  $\text{CDCl}_3$  were better swelling solvents than  $\text{D}_2\text{O}$ , DMF, methanol, benzene, or toluene. For the aliphatic–aromatic potato biopolyester suberin in polysaccharide cell walls, only  $\text{DMSO-}d_6$  yielded well-resolved HR-MAS NMR spectra spanning several spectral regions. As detailed later, whole soil HR-MAS NMR spectra acquired in contrasting solvents can be used to favor polar compounds at the soil–water interface or nonpolar compounds at more buried locations<sup>17</sup>; similar strategies could be useful to swell particular polymeric or networked regions within a plant or soil assembly. Mixed solvents are expected to do a complete job of swelling a sample that contains chemical moieties with a wide range of polarities, although we observed no improvements for, e.g.,  $\text{DMSO-}d_6$  with  $\text{CDCl}_3$  or  $\text{CD}_3\text{OD}$  with benzene.

**Swelling Protocol.** A rough measure of swelling efficacy can be made by immersing a given mass of solid sample in each of several solvents and comparing the volumes of the precipitates at equilibrium in closed containers,<sup>37</sup> although this procedure cannot reveal which constituents of a complex soil or plant material are swollen or inaccessible to solvent. NMR samples may be prepared by swelling the solid of interest in an excess volume of solvent, with vigorous stirring or bath sonication, for

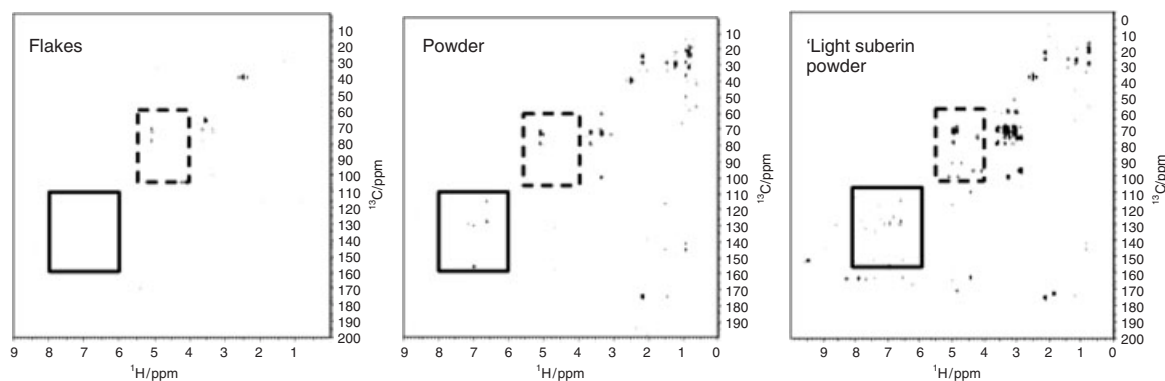


**Figure 4.** 750 MHz  $^1\text{H}$  HR-MAS-gHMBC NMR spectra of suberized potato wound periderm in flaked, powder, and 'light' forms, each swelled in  $\text{DMSO-}d_6$  and run at  $50^\circ\text{C}$ . Suberized tissue, either as flakes or ground into a powder with a liquid  $\text{N}_2$ -cooled freezer mill, was treated with cellulase and pectinase as described earlier;<sup>54</sup> the 'light' designation refers to the floating solid layer obtained after centrifugation of powdered wound periderm. The data were obtained with  $10.000 \pm 0.001$  kHz MAS and  $40 \text{ G cm}^{-1}$  magic-angle PFGs using a Bruker HR-MAS probe; the 65 ms defocusing period in HMBC was optimized for a multiple-bond  $^1\text{H}$ - $^{13}\text{C}$  scalar coupling of 8 Hz

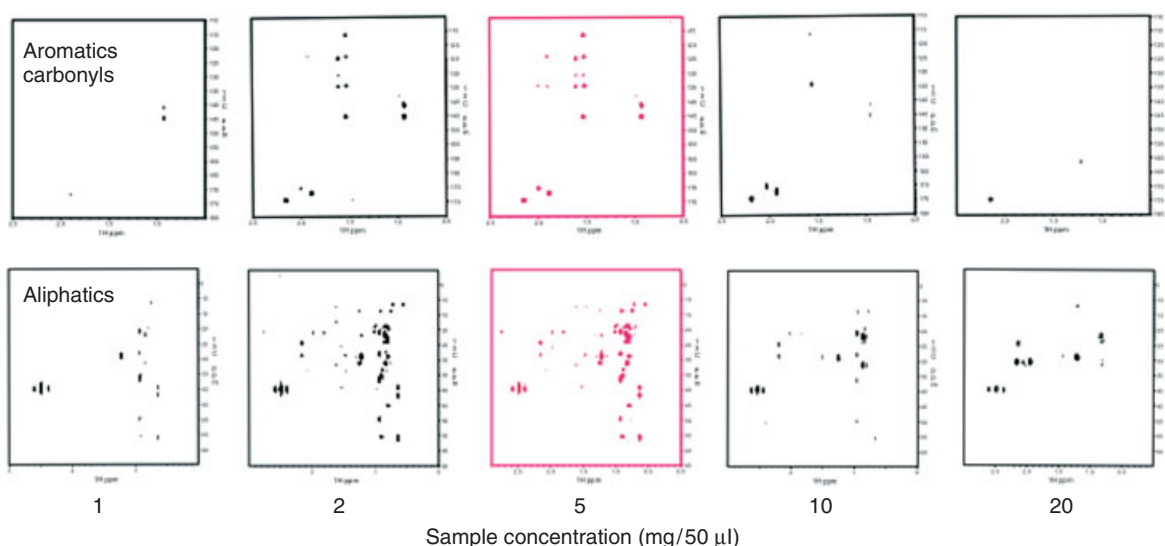


**Figure 5.** 750 MHz  $^1\text{H}$  HR-MAS-gHMBC NMR spectra of intracellular adhesion-strengthened ('hardened') potato tissue swelled in  $\text{DMSO-}d_6$  at different concentrations and run at  $50^\circ\text{C}$ . The data were obtained with  $6.00 \pm 0.001$  kHz MAS and  $40 \text{ G cm}^{-1}$  magic-angle PFGs; the 65 ms defocusing period was optimized for a multiple-bond  $^1\text{H}$ - $^{13}\text{C}$  scalar coupling of 8 Hz

>24 h at ambient or elevated temperature. Then, excess solvent is removed by filtration, and the swollen material is packed immediately into the rotor (or rotor insert). Alternatively, when the amount of sample is limited, it is possible to mix the solid with solvent inside the 40 to 50  $\mu\text{l}$  rotor, allow swelling in situ, and then mix further during MAS-assisted acquisition of the NMR spectra. Liquid-tight sample cells are essential to maintain the solid-to-solvent ratio for the duration of one or more HR-MAS NMR measurements.

*Choice of Temperature.* Certainly molecular mobility is enhanced as the temperature rises, so provided that the solid of interest is chemically stable and the solvent remains in the liquid phase, more complete motional averaging should make it easier to achieve liquid-like spectral resolution with MAS methods. In addition, elevated temperatures will

benefit experiments such as HMBC by lengthening  $T_2$  of the liquid-like molecular moieties, a trend confirmed for our potato wound suberin samples at 25 vs  $50^\circ\text{C}$  (data not shown). However, raising the temperature of these samples is also likely to compromise the overall spectral resolution by increasing resonance contributions from the solid-like chemical moieties (as proposed earlier in connection with particle size and concentration considerations). In practice, it is often necessary to simply evaluate a series of  $^1\text{H}$  spectra at different temperatures empirically and then proceed with more comprehensive 2-D experiments.

### Spectral Acquisition Strategies for Swelled Solids

In addition to the precautions recommended earlier for sample preparation, care is required with the choice of acquisition

**Table 1.**  $^1\text{H}$  spin relaxation times for melanin samples<sup>a</sup>

Chemical shift (ppm)	$T_1$ (s)		$T_2$ (ms)	
	Unground	Ground	Unground	Ground
0.84	1.7	1.0	162	171
1.23	0.9	0.7	79	89
2.16	1.0	0.6	158	119
5.30	1.2	0.7	40	35
5.31	1.2	0.8	42	45

<sup>a</sup>*Cryptococcus neoformans* melanin ghosts were prepared from [2,3- $^{13}\text{C}$ ]-L-dopa and [U- $^{13}\text{C}$ ]-glucose as described earlier.<sup>33</sup> 'Ground' denotes 20 min of manual grinding with a mortar and pestle. Errors are estimated as 10% based on repeated trials.

**Table 2.**  $^{13}\text{C}$  spin relaxation times for melanin samples<sup>a</sup>

Chemical shift (ppm)	$T_1$ (s)		$T_2$ (ms)	
	Unground	Ground	Unground	Ground
28.8	1.1	1.0	5.0	62
28.6	1.2	1.0	1.3	23
129.5	1.6	1.3	2.4	30

<sup>a</sup>*Cryptococcus neoformans* melanin ghosts were prepared from [2,3- $^{13}\text{C}$ ]-L-dopa and [U- $^{13}\text{C}$ ]-glucose as described earlier.<sup>33</sup> 'Ground' denotes 20 min of manual grinding with a mortar and pestle. Errors are estimated as 15% based on repeated trials.

conditions for HR-MAS NMR experiments on swelled solids. By monitoring the impact of MAS and specific spin rate on  $^1\text{H}$  NMR spectra for plant and soil samples, it is possible to deduce the factors determining the observed linewidth and to devise strategies for optimization. In addition, it is possible to improve spectral quality for many solvent-swelled biomaterials through the use of solvent suppression, diffusion editing,<sup>38</sup> and spin-echo techniques that are standard for HR-MAS NMR of aqueous-based tissue samples.<sup>21</sup>

**Choice of Magic-angle Spinning Rate.** Although  $^1\text{H}$  NMR spectra of solvent-swelled biopolymer samples are typically broad ( $\Delta\nu_{1/2} \geq 100$  Hz) in the absence of MAS, trials conducted with MAS at 1–10 kHz evidence dramatic resolution improvements for lime cutin<sup>16,24</sup> (Figures 1 and 2), potato tissues,<sup>32</sup> and fungal melanins<sup>18,33</sup> that are essentially complete at modest spin rates of  $\sim 2.5$  kHz. These observations suggest that dipole–dipole interactions are reduced (or abolished) for any molecular entities that are exposed to the solvent and thus able to tumble more freely. Any remaining dipole–dipole couplings could then be averaged by MAS; however, the rate requirements should depend on the size of the residual coupling for a given pair of proton spins. As modest MAS rates often serve to improve spectral resolution for all  $^1\text{H}$  resonances in these plant samples, it is likely instead that swelling allows complete motional averaging and that MAS serves to remove magnetic susceptibility anisotropy.<sup>13</sup> The  $^1\text{H}$  resonance linewidths nonetheless remain somewhat broader, for instance, for solvent-swelled lime fruit cutin than a soluble trimer constituent trimer (Figure 3); we attribute this trend to

chemical-shift heterogeneity—partially overlapped resonances from a greater number of chemically similar groups in the intact biopolymer as compared with a particular aliphatic trimer.

Can we benefit by using higher MAS rates? As indicated earlier, if residual dipolar couplings are removed by solvent swelling and magnetic susceptibility anisotropy is abolished by MAS, then increasing the spin rate will produce no further line narrowing. Nonetheless, it may be advantageous to spin at, say, 10 kHz in order to place spinning sidebands outside the spectral window of interest,<sup>17</sup> provided that sample integrity is not compromised. Although current commercial HR-MAS probe specifications include  $^1\text{H}$  linewidths of 1.5/15/25 Hz at 50/1/0.05% height for solution-state standards such as chloroform in acetone, half-height linewidths of 10–1500 Hz are observed in practice for amorphous swelled-solid environmental materials in which chemically similar constituents exhibit overlapping resonances.

Do FastMAS<sup>®</sup>, UltraFastMAS<sup>®</sup>, or Very High Speed DVT MAS<sup>®</sup> probe technologies offer an alternative to doing HR-MAS NMR experiments on solvent-swelled environmental materials? If the goal is characterization of soil–aqueous interfaces<sup>17</sup> or urban surface films,<sup>39</sup> then swelling followed by HR-MAS NMR offers a measure of spatial selectivity that would be lost by FastMAS experiments on dry samples. If the target is a region of suberized plant cell walls that remains rigid because of dense crosslinking or obstructed solvent accessibility, then FastMAS methods may be the only NMR-based investigative options that can augment the organizational and molecular information forthcoming from FT-infrared (IR) and X-ray diffraction measurements. Even so,  $^1\text{H}$  FastMAS experiments are likely to exhibit limited spectral resolution, as illustrated by aryl and alkyl functional groups in a pyrogenic carbon residue (Figure 6).<sup>40</sup>

**Water Suppression.** In the presence of an abundance of residual  $^1\text{H}$  nuclei from the swelling solvent, the spectrum of the sample of interest will be dominated by solvent signals; nuclear spins that resonate at similar chemical shifts will also be lost in the shoulders of the solvent signal. The techniques for removal of interfering solvent resonances from solution-state NMR spectra, which are often suitable for environmental or biomedical HR-MAS NMR applications, run the gamut from simple presaturation to WATERGATE, excitation sculpting, and presaturation utilizing relaxation gradients and echoes (PURGE).<sup>21,22</sup>

**Spectral Editing for Mobile or Immobilized Environmental Constituents.** The use of CPMG spin-echo sequences (CPMG  $T_2$  filters)<sup>31</sup> is well established for the suppression of broad NMR signals that arise from rapidly relaxing immobilized species such as human bone; the offending species have also included polymer resins in HR-MAS NMR spectra of covalently bound combinatorial peptide libraries,<sup>13</sup> and intact organs in HR-MAS NMR experiments designed to observe small-molecule metabolites.<sup>21</sup> Figure 7 shows a striking example of the resulting spectral improvement for a whole soil environmental sample,<sup>17</sup> in which the broad background signals were attributed either to macromolecules or to

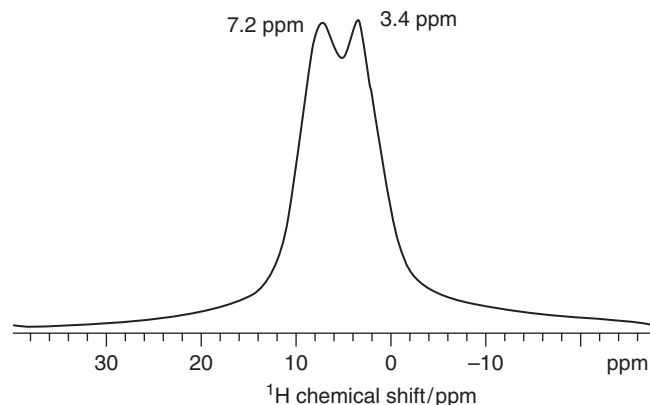


**Figure 6.** 600 MHz  $^1\text{H}$  NMR spectrum obtained at a spinning speed of  $35.00 \pm 0.01$  kHz using a Varian (Agilent) FastMAS probe for pyrogenic organic matter from ponderosa pine wood, showing spectral features from oxygenated aliphatic and aromatic moieties at 3.4 and 7.2 ppm, respectively.<sup>40</sup> (Reproduced with permission from Ref. 40. © Elsevier, 2012)

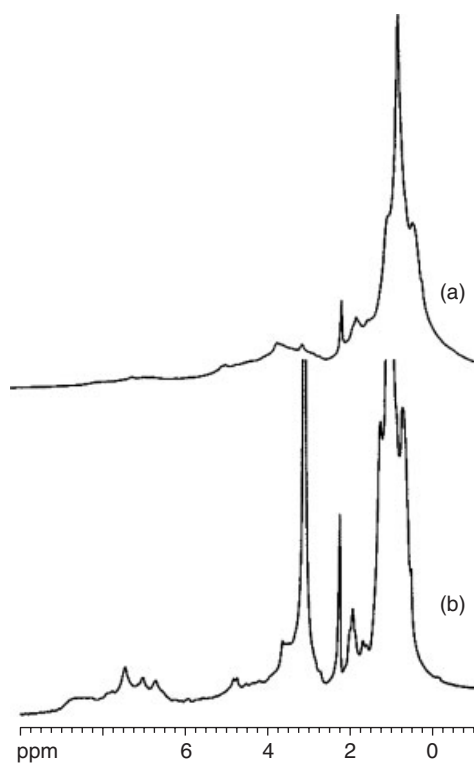


**Figure 7.** 600 MHz  $^1\text{H}$  HR-MAS spectra of a whole forest soil swelled in  $\text{DMSO-}d_6$ , obtained with a Bruker HR-MAS probe.<sup>17</sup> (a) 12 kHz spinning with presaturation of water present in the solvent; (b) 12 kHz spinning (with partial presaturation of the water signal at 3.3 ppm) and  $T_2$  filtering achieved by insertion of a CPMG sequence with 1.2 ms delays between  $180^\circ$  pulses before NMR signal acquisition. (Reprinted with permission from A. J. Simpson, W. L. Kingery, D. Shaw, M. Spraul, E. Humpfer, P. Dvortsak, *Envir. Sci. Tech.*, **2001**, 35, 3321. Copyright 2001 American Chemical Society)

components associated with mineral surfaces or paramagnetic substances. Thus, such  $T_2$  filter methods are efficacious when the investigator wishes to observe relatively mobile species present in an immobilized matrix. The chemical information

forthcoming from such investigations is summarized in the section titled 'Representative Applications to Environmental Science'.

Conversely, an editing strategy that favors rigid constituents has been implemented for wheat grass residues from simulated degradation studies using  $^1\text{H}$  diffusion-gated NMR experiments.<sup>38,41</sup> Using bipolar pulse pairs refined in connection with diffusion-ordered 2-D NMR spectroscopy, it was possible to remove mobile components from the spectra of grass blades (Figure 8), demonstrating that the sharp carbohydrate resonances appearing in the  $^1\text{H}$  HR-MAS NMR spectrum after a month's microbial decomposition come from chemical entities displaying rapid translational diffusion. A more complete discussion of the chemical transformations appears in the section titled 'Representative Applications to Environmental Science'.

#### Hardware for HR-MAS NMR Experiments

Each of the major commercial NMR vendors offers specialized probes for HR-MAS; no additional high-power amplifiers are required, and probes are currently in operation at  $^1\text{H}$  frequencies up to 900 MHz. As noted earlier, many MAS probes have similarly excellent lineshape specifications to solution-state probes, although attainable resolution is often limited by the heterogeneity or motional freedom of the environmental sample. Currently available HR-MAS probes are typically outfitted with a  $^2\text{H}$  field-frequency lock and PFG capabilities to allow for tailored solvent suppression and coherence selection in multidimensional experiments. The range of typical probe temperatures is typically  $20\text{--}50^\circ\text{C}$ , which is sufficient for examination of most environmental and biomedical samples of interest. Inverse detection and three-channel capabilities are available; these features make it possible, for instance, to collect 2-D  $^1\text{H}\text{--}^{13}\text{C}$  and  $^1\text{H}\text{--}^{15}\text{N}$  data with ease, particularly if the sample is present at high concentration in natural abundance or is enriched with NMR-active isotopes. Typical rotor diameters are 4–5 mm, with spinning capabilities of 2–15 kHz depending on the rotor material and other design parameters. Although rotors can be costly to purchase, many vendors offer

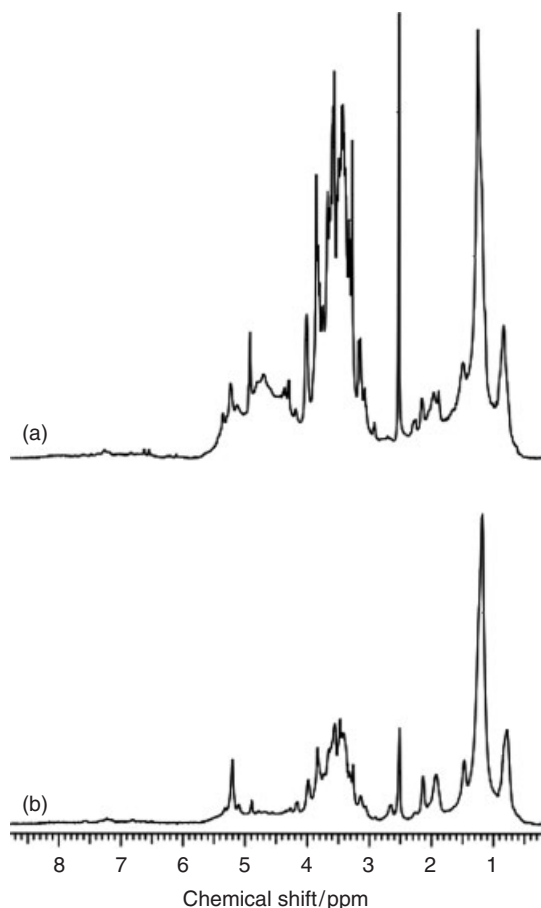


**Figure 8.** 500 MHz  $^1\text{H}$  HR-MAS spectra of wheat grass blades swelled in  $\text{DMSO-}d_6$  after 1 month of modeled environmental degradation.<sup>41</sup> (a) Standard HR-MAS with a Bruker probe at 10 kHz; (b) HR-MAS at 10 kHz with diffusion editing. (Reproduced with permission from Ref. 41. © Elsevier, 2006)

inexpensive inserts that also ensure sealing of wet samples. It should also be noted that HR-MAS NMR experiments can be performed in a recently introduced probe for comprehensive multiphase NMR spectroscopy.<sup>42</sup> The reader is referred to the vendor websites and literature for additional information.

### Representative Applications to Environmental Science

Although HR-MAS NMR applications are presented elsewhere in this *encyclopedia*, in this section, we highlight both the methodology and caveats related to such environmental science investigations. While 1-D HR-MAS NMR procedures have been described earlier, we now emphasize the use of HR-MAS in conjunction with various 2-D NMR methods (COSY, TOCSY, HMQC, HMBC, NOESY, HMQC-TOCSY, etc.) to delineate structurally informative through-bond and through-space interactions for plant and soil systems. Comparisons are made with solution- and solid-state NMR investigations of representative environmental materials, including critical assessments of the capabilities of HR-MAS NMR to provide reliable and otherwise unavailable structural or dynamic information.

### Soil Science: HR-MAS NMR at Solid–Solvent Interfaces

Whole soil is comprised of soluble, solid, and swellable constituents, each requiring a tailored spectroscopic approach for molecular characterization. The first  $^1\text{H}$  HR-MAS NMR experiments of these complex systems<sup>17</sup> were shown to provide otherwise inaccessible information regarding molecular structure at the solid–aqueous interface. HR-MAS NMR experiments can avoid concerns about artifacts associated with the spectra of soluble extracts, and they also have the potential to refine generic compositional information derived from CP-MAS  $^{13}\text{C}$  NMR of powdered samples.<sup>43</sup> The spectra exhibit relatively sharp resonances and good sensitivity, particularly if presaturation is used to attenuate the solvent signal and spin-echo filtering is used to remove broad contributions from rapidly relaxing high-molecular-weight and paramagnetic species. The  $^1\text{H}$  HR-MAS NMR data reflect the solvent-accessible components of the solid soil; independent examination of the supernatant verifies that the spectra contain no contributions from soluble constituents.

In  $\text{D}_2\text{O}$ , the observed chemical shifts implicate predominantly (oxy)aliphatic moieties, which were confirmed by 2-D MAS-TOCSY NMR (Figure 9) to arise from acids, esters, ethers, and sugars found previously in soil organic extracts. Additional resonances from aromatic structures are evident when the sample is swelled in  $\text{DMSO-}d_6$ , a ‘penetrating’ solvent for both hydrophilic and hydrophobic domains that may also break hydrogen bonds. The inference drawn from such studies is that aliphatic moieties are most involved in the binding of the aqueous-phase contaminants and heavy metals that raise environmental concerns. By contrast, the aromatic moieties may exist in hydrophobic environments such as phyllosilicate clays.

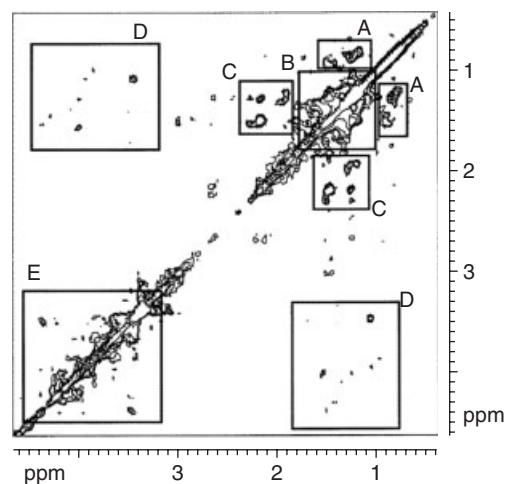


**Figure 9.** Aliphatic region of a 600 MHz 2-D HR-MAS-TOCSY spectrum recorded for a whole soil sample swelled in  $\text{D}_2\text{O}$ , showing scalar couplings between pairs of  $\text{CH}_3$ ,  $\text{CH}_2$ , and sugar groups designated by the letters A–E.<sup>17</sup> (Reprinted with permission from A. J. Simpson, W. L. Kingery, D. Shaw, M. Spraul, E. Humpfer, P. Dvortsak, *Envir. Sci. Tech.*, **2001**, 35, 3321. Copyright 2001 American Chemical Society)



### Environmental Carbon and Nitrogen Cycling: HR-MAS NMR for Chemical Conversions

HR-MAS NMR approaches also have excellent potential for studies of terrestrial plant litter decomposition, a process in which a variety of carbohydrates, tannins, proteins, lignins, waxes, and cutins have differing susceptibilities to environmental degradation and capabilities for carbon or nitrogen sequestration.<sup>44</sup> An example that illustrates several useful techniques for such work is provided by Kelleher *et al.*,<sup>41</sup> who devised a model system to monitor the degradation of lodgepole pine (*Pinus contorta*) and Western wheat grass (*Agropyron smithii*) plant materials during a year's time.

<sup>1</sup>H HR-MAS NMR provided sufficient spectral resolution to identify regions for aromatic, carbohydrate, oxymethine, oxymethylene, methylene, and methyl groups, and as described earlier, the rigid moieties could be selected by a diffusion-edited experiment.<sup>38</sup> By enriching these materials in the <sup>13</sup>C isotope, the investigators were able to observe <sup>13</sup>C spectra directly, obtaining the superior chemical-shift dispersion and resolution illustrated in Figure 10. Enrichment with both <sup>13</sup>C and <sup>15</sup>N also facilitated acquisition of 2-D heteronuclear single-quantum coherence (HSQC) NMR spectra, further improving

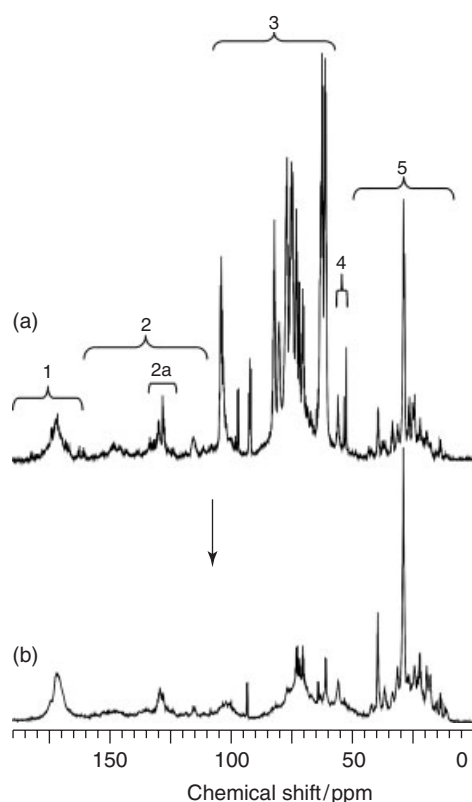


**Figure 10.** <sup>13</sup>C HR-MAS spectra of wheat grass leaves obtained with a spinning rate of 10 kHz at an NMR frequency of 125 MHz, showing chemical differences between materials that are fresh (a) and decomposed for 12 months (b). The numbered spectral regions were assigned structurally by analogy with published literature to carbonyls (1), aromatic and doubly bonded moieties (2), carbohydrates (3), methoxyls (4), and aliphatics (5).<sup>41</sup> (Reproduced with permission from Ref. 41. © Elsevier, 2006)

the resolution of the <sup>1</sup>H spectra and allowing identification of covalently bound <sup>1</sup>H–<sup>13</sup>C and <sup>1</sup>H–<sup>15</sup>N structural fragments.

In the wheat grass, for instance, fresh blades were demonstrated to consist of predominantly rigid (macromolecular) components, whereas decomposed materials had a greater proportion of mobile (small) carbohydrate units that also displayed sharper resonances. Conversely, the relative intensity of aliphatic resonances increased with time, likely reflecting the more modest decomposition rates of cutin and wax components. Notably, it was possible to demonstrate disappearance and buildup of particular compound classes by analysis of the HR-MAS-assisted <sup>1</sup>H–<sup>13</sup>C HSQC NMR fingerprints of the pine needle samples: cross-peaks from tannins had nearly disappeared after 12 months, whereas features attributable to triterpenoids became more prominent in the spectra because of their evident recalcitrance. Finally, HR-MAS <sup>1</sup>H–<sup>15</sup>N HSQC NMR of the pine needles and stem/root materials revealed a decrease in protein that was accompanied by buildup of as-yet-unidentified nitrogen-containing molecules that could originate either from the fresh plants or new microbe-assisted synthesis. Although it remains difficult to discriminate quantitatively between swelled and solid materials and to identify specific chemical compounds as well as compound classes involved in particular transformations, the superior resolution and covalent bonding information provided by HR-MAS NMR makes it a powerful tool on its own and as a complement to CP-MAS approaches for associated solids.

### Plant Protective Biopolymers: nD HR-MAS NMR for Macromolecular Architecture

**HR-MAS-HMQC NMR of Citrus Fruit Cutins: Capabilities and Caveats.** The 1-D <sup>1</sup>H HR-MAS spectra shown in Figures 1 and 2 display dramatic NMR resolution enhancement of the lime fruit cutin biopolymer with solvent swelling. Moreover, 2-D data such as the well-resolved <sup>1</sup>H–<sup>13</sup>C HMQC NMR spectra in Figure 3 offer the potential for monitoring the mild chemical or enzymatic transformations used to produce oligomeric fragments that preserve elements of the biopolymer architecture.<sup>45</sup> The HMQC NMR spectrum of the swelled-solid residue in Figure 3(c) suggests loss of some aliphatic chain groups but resembles the original polyester as expected, as only ~20% of the lime cutin is broken down by this particular treatment. Moreover, the highlighted regions of the <sup>1</sup>H–<sup>13</sup>C HMQC NMR fingerprints shown in Figure 3(a) and (b) offer insight into the chemical transformations that accompany depolymerization: the CH<sub>2</sub>OR group of the cutin (61, 3.4 ppm) is cleaved to CH<sub>2</sub>OH (63, 3.6 ppm) in a major soluble product. The oligomer also shows new CH<sub>3</sub>CH<sub>2</sub>OC=O (60, 4.1 ppm) and CH<sub>3</sub>CH<sub>2</sub>OC=O (14, 1.2 ppm) groups consistent with termination by an ethyl ester<sup>24,46</sup> and was subsequently elucidated as a linear trimer ester of 10-oxo-16-hydroxyhexadecanoic acid using traditional solution-state NMR and mass spectrometry methods.<sup>45</sup>

However, neither midchain alcohol nor ester groups are observed in 2-D HR-MAS NMR spectra of the cutin polymer or the unreacted residue (Figure 3b and c),<sup>24</sup> despite evidence for such structural features in both soluble monomeric breakdown

products<sup>47,48</sup> and intact dry solids examined by CP-MAS <sup>13</sup>C NMR.<sup>25</sup> In retrospect, then, the 1-D HR-MAS <sup>1</sup>H spectral comparisons in Figures 1 and 2 do not provide sufficiently stringent support for the completeness of solvent swelling in this material; the same factors that pose challenges for polymer degradation<sup>49</sup> are likely to defeat efforts to swell the samples with DMSO-*d*<sub>6</sub>.

**HR-MAS-HMQC with HR-MAS-COSY NMR of Potato Tuber Stress Response: Tracing Polysaccharide Architecture.** A better prospectus for macromolecular investigation is offered by potato biopolymers formed on cell-wall surfaces in response to environmental stresses such as wounding in order to prevent dehydration and microbial invasion. Figure 11 illustrates the coordinated use of 2-D HR-MAS-assisted HMQC with COSY NMR experiments to make structural assignments for the cell-wall polysaccharides protected by the aliphatic–aromatic polyester suberin. For these DMSO-*d*<sub>6</sub>-swelled samples, resolution is excellent and all of the expected functional groups are swelled successfully following the sample preparation guidelines outlined earlier. To assign the polysaccharide resonances, the <sup>1</sup>H peaks at 4.4, 5.4, and 5.5 ppm were first identified tentatively as hydroxyl substituents on sugar rings of the polysaccharides, based on their chemical-shift values and susceptibility to exchange with D<sub>2</sub>O. Using a strategy similarly to that reported in a prior investigation of intracellular adhesion-strengthened potato tissues,<sup>32</sup> these sugar hydroxyl assignments were confirmed and linked to their respective sugar ring positions by comparing the through-bond connectivities in double-quantum-filtered (DQF) COSY and <sup>1</sup>H–<sup>13</sup>C HMQC experiments (Table 3). As reported for the texture-spoiling potato polymer described earlier,<sup>32</sup> the lack of a hydroxyl group at ring position 2 suggests that other parts of the biopolymer are attached at that site.

**HR-MAS-HMBC NMR of Potato Tuber Stress Response: Mapping Inter-domain Connections.** How are the aliphatic and aromatic domains of the suberin polyester linked together, and

what is the nature of the covalent architecture or noncovalent associations that occur with the underlying cell-wall polysaccharides? Till date, proposals of covalent bonding within this assembly have relied on indirect evidence from <sup>13</sup>C spin–lattice relaxation and <sup>13</sup>C–<sup>13</sup>C spin diffusion experiments.<sup>50,51</sup> Current solid-state NMR protocols for measuring carbon–carbon spatial proximities or through-bond connections require isotopic enrichment and may display limited spectroscopic resolution for amorphous materials. By contrast, a measure of detail regarding inter-domain connections can be derived from HR-MAS-assisted <sup>1</sup>H–<sup>13</sup>C HMBC NMR experiments if the plant tissue samples are swelled in DMSO-*d*<sub>6</sub> to enhance molecular motions (Figure 12).

Firstly, the spectrum shows multiple-bond connections between carboxyl carbons and aliphatic chain methylene groups (dashed rectangle), as expected from longstanding observations of C<sub>18</sub> hydroxy fatty acid monomer building blocks within the aliphatic domain of the potato suberin polyester.<sup>47</sup> Secondly, HMBC demonstrates long-range bonding between aliphatic and aromatic groups (solid rectangle), consistent with suberin's proposed aliphatic–aromatic polyester structure.<sup>47,52,53</sup> Finally, the contour plot shows connections between aliphatic and carbohydrate resonances (solid circle), augmenting NOESY and TOCSY evidence of their proximities (data not shown) and offering the first direct evidence of covalent linkages between the protective suberin polymer and the cell-wall periderm (phellem) tissues. Efforts to enhance the sensitivity and completeness of these encouraging experiments are ongoing.

**Table 3.** NMR resonance assignments for carbohydrate signals in suberized potato wound periderm tissues

Glucose structural position	1	2	3	4	5	6
<sup>1</sup> H shift (ppm)	5.01, 5.04	3.35	3.66	3.31	3.60	3.55, 3.67
<sup>13</sup> C shift (ppm)	99.9	78.7	72.7	71.7	71.4	60.1

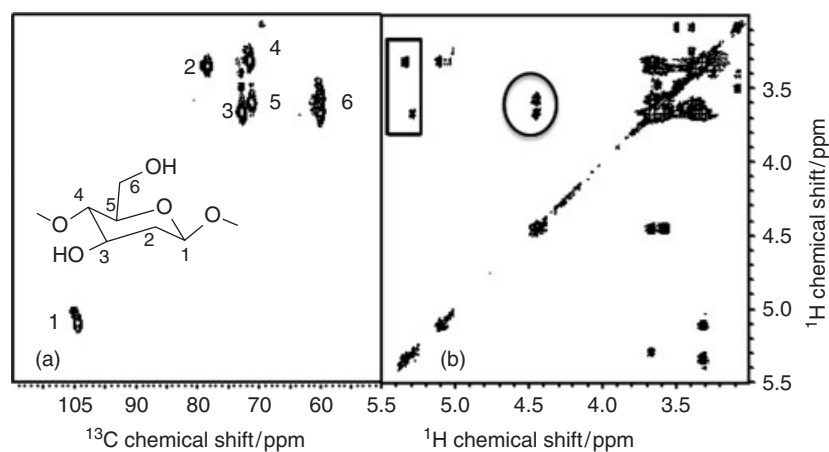


**Figure 11.** Upfield portion of the HR-MAS-assisted <sup>1</sup>H–<sup>13</sup>C gHMQC (a) and <sup>1</sup>H–<sup>1</sup>H COSY (b) contour plots from NMR experiments conducted on DMSO-*d*<sub>6</sub>-swelled suberized potato wound periderm at 50 °C, obtained with a proton frequency of 600 MHz and a spinning frequency of 3.000 ± 0.001 kHz. The highlighted COSY cross-peaks designate through-bond correlations between protons on the sugar rings and their attached OH groups; the HMQC correlations confirm the ring assignments and locate the hydroxyl substituents (Table 3)

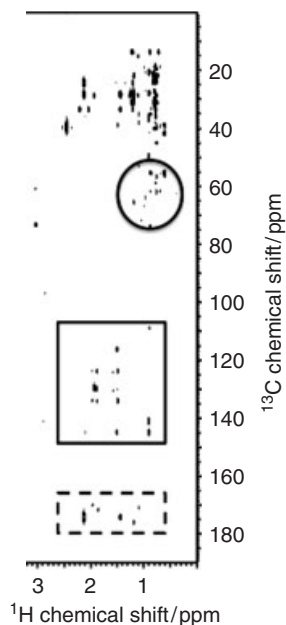


**Figure 12.** Upfield portion of the contour plot from 750 MHz HR-MAS-gHMBC NMR of suberized potato wound periderm swelled in DMSO- $d_6$  at 50 °C, showing multiple-bond connectivities within the suberin aliphatic domain (dashed rectangle), between suberin aliphatic and aromatic domains (solid rectangle), and between the suberin aliphatics and cell-wall polysaccharides (solid circle). The data were obtained with  $10.000 \pm 0.001$  kHz MAS and  $40 \text{ G cm}^{-1}$  magic-angle PFGs; the 65 ms defocusing period was optimized for a multiple-bond scalar coupling of 8 Hz

## Conclusions

HR-MAS NMR techniques are well suited for atomic- and molecular-level investigations of heterogeneous environmental samples such as soils, plant biomass, protective plant biopolymers, and urban surface films. With suitable optimization of sample preparation and data acquisition, this technology can be coupled usefully with a wealth of powerful 1-D spectral editing methods and multidimensional structure elucidation experiments and is generally applicable to NMR-active nuclei present at natural abundance. Neither soil or tissue extraction is required nor is it necessary to subject the macromolecular entities of interest to chemical degradation. HR-MAS NMR can often provide a unique route to inaccessible but functionally important information about intractable amorphous solids, solid–solvent interfaces, and chemical transformations of importance to environmental science and metabolic engineering.

## Acknowledgments

The work presented herein was supported by grants from the National Science Foundation (MCB-0843627, MCB-0741914, and DEB-1127253), the National Institutes of Health (R01-AI052733), and the US–Israel Binational Agricultural Research and Development Fund (USIS-3368-02). NMR resources were supported by the College of Staten Island, the City College

of New York, and the CUNY Institute for Macromolecular Assemblies. Additional infrastructural support was provided by NIH 2G12RR03060 from the National Center for Research Resources and 8G12MD007603 from the National Institute on Minority Health and Health Disparities. Prof. R.E.S. is a member of the New York Structural Biology Center (NYSBC); data collected at the NYSBC was made possible by a grant from NYSTAR. We gratefully acknowledge Drs Hsin Wang and Boris Itin for technical assistance with the NMR experiments; Dr Subhasish Chatterjee and Ms Lauren Gohara also provided patient assistance with the preparation of this article.

## Biographical Sketch

Ruth E. Stark was born in 1950. She obtained her PhD, 1977, in physical chemistry at the University of California (San Diego), USA. She was an NIH postdoctoral fellow at MIT, 1977–1979. She has worked as assistant professor at Amherst College, 1979–1985; associate to distinguished professor at the City University of New York (CUNY), 1985–present; director of the CUNY Institute for Macromolecular Assemblies, 2003–present. She has authored more than 100 publications. Her current research interests are solid and solution NMRs with applications to molecular biophysics of lipid transport, structure and development of protective plant polymers, and molecular structure and assembly of fungal melanins.

Bingwu Yu was a postdoctoral fellow at CUNY.

Junyan Zhong was a postdoctoral fellow at CUNY.

Bin Yan was a postdoctoral fellow at CUNY.

Guohua Wu was a CUNY PhD student in the Stark Laboratory.

Shiyong Tian was a CUNY PhD student in the Stark Laboratory

## Related Articles

NMR Probes for Small Sample Volumes; High-resolution MAS for Liquids and Semisolids; Agriculture and Soils

## Further Reading

1. A. J. Simpson, M. J. Simpson, and R. Soong, *Environ. Sci. Technol.*, 2012, **46**, 11488.

## References

1. D. Doskocilova, D. D. Tao, and B. Schneider, *Czech. J. Phys.*, 1975, **B25**, 202.
2. D. Doskocilova, B. Schneider, and J. Jakes, *J. Magn. Reson.*, 1978, **29**, 79.
3. H. D. H. Stover and J. M. J. Frechet, *Macromolecules*, 1989, **22**, 1574.
4. W. T. Ford, S. Mohanraj, and H. Hall, *J. Magn. Reson.*, 1985, **65**, 156.
5. H. D. H. Stover and J. M. J. Frechet, *Macromolecules*, 1991, **24**, 883.
6. E. Oldfield, J. L. Bowers, and J. Forbes, *Biochemistry*, 1987, **26**, 6919.
7. J. Forbes, C. Husted, and E. Oldfield, *J. Am. Chem. Soc.*, 1988, **110**, 1059.
8. E. Krainer, R. E. Stark, F. Naider, K. Alagramam, and J. M. Becker, *Biopolymers*, 1994, **34**, 1627.
9. H. N. Halladay, R. E. Stark, S. Ali, and R. Bittman, *Biophys. J.*, 1990, **58**, 1449.
10. L. L. Holte and K. Gawrisch, *Biochemistry*, 1997, **36**, 4669.

11. W. L. Fitch, G. Detre, and C. P. Holmes, *J. Org. Chem.*, 1994, **59**, 7955.
12. R. C. Anderson, M. A. Jarema, M. J. Shapiro, J. P. Stokes, and M. Ziliox, *J. Org. Chem.*, 1995, **60**, 2650.
13. P. A. Keifer, L. Balthuis, D. M. Rice, A. A. Typiak, and J. N. Shoolery, *J. Magn. Reson. A*, 1996, **119**, 65.
14. W. E. Maas, F. H. Laukien, and D. G. Cory, *J. Am. Chem. Soc.*, 1996, **118**, 13085.
15. D. Moka, R. Vorreuther, H. Schicha, M. Spraul, E. Humpfer, M. Lipinski, P. J. Foxall, J. K. Nicholson, and J. C. Lindon, *J. Pharm. Biomed. Anal.*, 1998, **17**, 125.
16. R. E. Stark, B. Yan, A. K. Ray, Z. Chen, X. Fang, and J. R. Garbow, *Solid State Nucl. Magn. Res.*, 2000, **16**, 37.
17. A. J. Simpson, W. L. Kingery, D. Shaw, M. Spraul, E. Humpfer, and P. Dvorsak, *Environ. Sci. Technol.*, 2001, **35**, 3321.
18. S. Tian, J. Garcia-Rivera, B. Yan, A. Casadevall, and R. E. Stark, *Biochemistry*, 2003, **42**, 8105.
19. W. Li, *Analyst*, 2006, **131**, 777.
20. F. Bertocchi and M. Paci, *J. Agric. Food Chem.*, 2008, **56**, 9317.
21. J. C. Lindon, O. P. Beckonert, E. Holmes, and J. K. Nicholson, *Prog. Nucl. Magn. Reson. Spectrosc.*, 2009, **55**, 79.
22. A. J. Simpson, D. J. McNally, and M. J. Simpson, *Prog. Nucl. Magn. Reson. Spectrosc.*, 2011, **58**, 97.
23. R. E. Stark, B. Yan, and G. Wu, 40th Experimental NMR Conference, Orlando, FL, 1999, p 20.
24. X. Fang, F. Qiu, B. Yan, H. Wang, A. J. Mort, and R. E. Stark, *Phytochemistry*, 2001, **57**, 1035.
25. T. Zlotnik-Mazori and R. E. Stark, *Macromolecules*, 1988, **21**, 2412.
26. R. E. Stark, T. Zlotnik-Mazori, L. M. Ferrantello, and J. R. Garbow, *ACS Symp. Ser.*, 1989, **399**, 214.
27. J. R. Garbow and R. E. Stark, *Macromolecules*, 1990, **23**, 2814.
28. A. P. Deshmukh, A. J. Simpson, and P. G. Hatcher, *Phytochemistry*, 2003, **64**, 1163.
29. A. P. Deshmukh, A. J. Simpson, C. M. Hadad, and P. G. Hatcher, *Org. Geochem.*, 2005, **36**, 1072.
30. R. E. Hurd and B. K. John, *J. Magn. Res.*, 1991, **91**, 648.
31. J. Cavanagh, W. J. Fairbrother, A. G. Palmer III, M. Rance, and N. J. Skelton, *Protein NMR Spectroscopy: Principles and Practice*, 2nd edn, Academic Press: New York, 2007.
32. B. Yu, G. Vengadesan, H. Wang, L. Jashi, T. Yefremov, S. Tian, V. Gaba, I. Shomer, and R. E. Stark, *Biomacromolecules*, 2006, **7**, 937.
33. J. Zhong, S. Frases, H. Wang, A. Casadevall, and R. E. Stark, *Biochemistry*, 2008, **47**, 4701.
34. H. Z. Hill, *BioEssays*, 1992, **14**, 49.
35. K. G. Valentine, R. W. Peterson, J. S. Saad, M. F. Summers, X. Xu, J. B. Ames, and A. J. Wand, *Structure*, 2010, **18**, 9.
36. J. M. Kielec, K. G. Valentine, C. R. Babu, and A. J. Wand, *Structure*, 2009, **17**, 345.
37. I. Shomer, R. Vasiliver, and P. Lindner, *Carbohydr. Polym.*, 1995, **26**, 55.
38. D. Wu, A. Chen, J. Johnson, and S. Charles, *J. Magn. Reson. A*, 1995, **115**, 260.
39. A. J. Simpson, B. Lam, M. L. Diamond, D. J. Donaldson, B. A. Lefebvre, A. Q. Moser, A. J. Williams, N. I. Larin, and M. P. Kvasa, *Chemosphere*, 2006, **63**, 142.
40. S. Chatterjee, F. Santos, S. Abiven, B. Itin, R. E. Stark, and J. A. Bird, *Org. Geochem.*, 2012, **51**, 35.
41. B. P. Kelleher, M. J. Simpson, and A. J. Simpson, *Geochim. Cosmochim. Acta*, 2006, **70**, 4080.
42. D. Courtier-Murias, H. Farooq, H. Masoom, A. Botana, R. Soong, J. G. Longstaffe, M. J. Simpson, W. E. Maas, M. Fey, B. Andrew, J. Struppe, H. Hutchins, S. Krishnamurthy, R. Kumar, M. Monette, H. J. Stronks, A. Hume, and A. J. Simpson, *J. Magn. Reson.*, 2012, **217**, 61.
43. M. A. Wilson, *NMR Techniques and Applications in Geochemistry and Soil Chemistry*, Pergamon Press: Oxford, UK, 1987.
44. P. Rovira and V. Ramo, *Geoderma*, 2002, **107**, 109.
45. S. Tian, X. Fang, W. Wang, B. Yu, X. Cheng, F. Qiu, A. J. Mort, and R. E. Stark, *J. Agric. Food Chem.*, 2008, **56**, 10318.
46. R. E. Stark and S. Tian, in *Biology of the Plant Cuticle*, eds M. Riderer and C. Muller, Blackwell Publishing Co: Oxford, UK, 2006, 126.
47. P. E. Kolattukudy, *Adv. Biochem. Eng. Biotechnol.*, 2001, **71**, 1.
48. T. J. Walton, *Meth. Plant Biochem.*, 1990, **4**, 105.
49. A. K. Ray and R. E. Stark, *Phytochemistry*, 1998, **48**, 1313.
50. R. E. Stark and J. R. Garbow, *Macromolecules*, 1992, **25**, 149.
51. B. Yan and R. E. Stark, *J. Agric. Food Chem.*, 2000, **48**, 3298.
52. M. A. Bernards, *Can. J. Bot.*, 2002, **80**, 227.
53. J. Graca and S. Santos, *Macromol. Biosci.*, 2007, **7**, 128.
54. R. A. Pacchiano, W. Sohn, V. L. Chlanda, J. R. Garbow, and R. E. Stark, *J. Agric. Food Chem.*, 1993, **41**, 78.